



Structural Topology Optimization of Brake Disc Using the Equivalent Moving Load Method

Shengfang Zhang, Jian Yin, Yu Liu*, Fujian Ma, Zhihua Sha & Dapeng Yang

School of Mechanical Engineering, Dalian Jiaotong University,
No. 794 Huanghe Road, Shahekou, Dalian 116028, China
*E-mail: liuyu_ly12@126.com

Abstract. During the braking process, the brake disc is subjected to the moving load. The process-point of the moving load moves along a certain trajectory, which makes it difficult to design the brake disc structure by using a traditional topology optimization method. The novel Equivalent Moving Load (EML) method proposed in this paper aims to solve this problem. According to the principle of continuous photographing technology, a mathematical model was established by using the round inward polygonal approximation algorithm. The EML method equalizes the continuous dynamic load action to many finite working conditions by geometric approximation. These working conditions are placed along the trajectory. The structure of the brake disc is then optimized by the EML method. Additionally, the influence of the layout style of the brake pads and the total number of working conditions on the optimization result are discussed in this paper. The optimization results showed that the new structure is a three-annulus structure. The weight of the new structure is reduced by 57.95% compared to the initial structure by structural topology optimization using the EML method. It was proved that structural topology optimization using the EML method is efficient in optimizing a structure subjected to dynamic load.

Keywords: *brake pad; brake disc; disc brake; equivalent moving load method; topology optimization.*

1 Introduction

Topology optimization is a mathematical method that optimizes material distribution within a given area based on given load conditions, constraints and performance requirements. When Bendsoe, *et al.* proposed the homogenization method in 1988, the topology optimization of continuum structures was born [1]. At present there are many topology optimization methods for continuum structures, including the homogenization method [2], the level set method [3], the evolutionary structural method [4], and the variable density method [5]. The research scope of topology optimization has been expanded based on these methods, from a single objective function to multi-objective functions and from a single condition to multiple conditions [6,7]. Based on the surrogate model technology, Qu, *et al.* have proposed an optimization design method of complex

structures; the method was applied to the design optimization of a ventilated disc brake [8].

Guo, *et al.* established a maximum braking torque optimization mathematical model and then used MATLAB optimization solution. The results showed that the disc brake's performance was improved [9]. However, the above studies mainly paid attention to structures with fixed loads. If these loads are transient, using a traditional method may not be effective. During the braking process, brake pads are pushed by the brake pressure to move to the brake disc until they make contact with the brake disc and the friction on both sides of the brake disc makes the rotation speed decrease. The magnitude and the process-point of contact pressure and the friction vary with the rotation of the brake disc. Therefore, the contact pressure and the friction belong to the moving load. Several researchers have studied structure optimization with dynamic loads. Zhang, *et al.* investigated topology optimization of a piezoelectric actuator/sensor coverage attached to a thin-shell structure and proposed a method to complete the layout design of the actuator/sensor layers attached to a thin-shell structure subject to dynamic excitation, in particular from impact forces [10]. Ivarsson, *et al.* implemented a transient finite strain viscoplastic model in a gradient-based topology optimization framework to design impact-mitigating structures [11]. Liu, *et al.* proposed an efficient approach for uncertain topology optimization in which the uncertain optimization problem is equivalent to that of solving a deterministic topology optimization problem with multiple load cases and considered the directional uncertainty of the applied loads [12,13]. Jeong, *et al.* developed a new layout optimization method based on the Equivalent Static Load (ESL) method to consider high-cycle fatigue constraints that occur due to variable amplitude mechanical loading [14].

The ESL method is a structural optimization method that can consider other methods than linear static analysis. ESLs are loads that generate the same response field of linear static analysis as that of nonlinear dynamic analysis at each time step. To deal with the dynamic characteristics in the optimization process, the equivalent static load method is employed to transform the dynamic topology optimization problem into a static one. Although the methods proposed in the above references can deal with the optimization of structures with dynamic loads, they are mainly concerned with the effect of the equivalent static load and the original dynamic load being the same. The equivalent moving load (EML) method proposed in this paper mainly considers three elements of the load, i.e. magnitude, direction and process-point. These three elements of the load influence the effect of the load. The EML method divides the dynamic process according to the trajectory of the load.

2 Proposal of the EML Method

2.1 Physical Model

The EML method is derived from the continuous photographing technology. When using the continuous shooting function of a camera to record the position of a moving object, the number of pictures taken per unit time is related to the frequency of pressing the shutter of the camera. The higher the frequency of pressing the shutter, the more pictures are taken and the more clearly the movement of the object is recorded.

Take a brake pad during the braking process as an example. If it is photographed 2 times in one rotation cycle, as shown in Figure 1(a), two shooting positions can be connected to form the diameter of the rotation trajectory circle. If it is taken 3 times in one rotation cycle, as shown in Figure 1(b), three shooting positions can be connected to form an inscribed equilateral triangle in the rotating trajectory circle. By analogy, if N photos are taken in one rotation cycle, N shooting positions can be connected to form an inscribed equilateral N -shape in the rotating trajectory circle. Thus, the high-speed movement process of the brake pad is equivalent to N static positions.

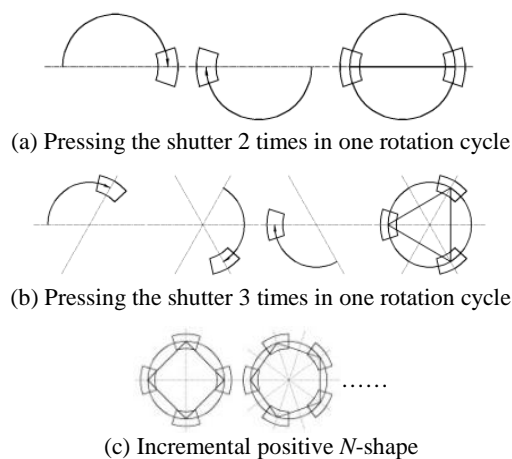


Figure 1 The principle of the continuous photographing technology.

2.2 Mathematical Model

The EML method was applied in this study to transform the continuous dynamic braking process into several equivalent working conditions.

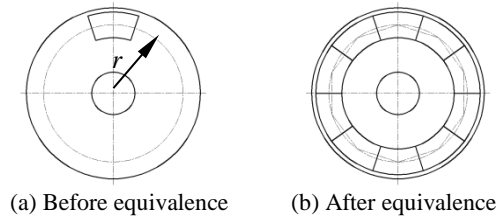


Figure 2 Schematic diagram of the EML method.

Figure 2(a) shows the actual braking process. The brake pad remains stationary; this is taken as the reference system. The brake disc rotates on a central axis and the moving trajectory of the central position on the brake pad is a circle with radius r . In Figure 2(b), the brake disc is seen as the reference system and remains stationary. The brake pad appears at different positions on the brake disc over time. The graphic formed by sequentially connecting the central positions is the inscribed regular polygon of the circle in Figure 2(b). An analogous mathematical description of the EML method can be performed by using the round inward polygonal approximation algorithm.

The trajectory formed by the movement of the central position on the brake pad relative to the brake disc is circular and the inscribed regular polygon is formed by sequentially connecting all the central positions after equivalence. The mathematical model can be established by using an inscribed regular polygon that approaches a circle. Suppose the radius of the circle is r , the edge number of the inscribed regular polygon is N and the degree of the circle's central angle on each edge is α_N . When N is given, $2\cos(2\pi/N)$ is a constant. In this case, the area of the sector and the triangle with the angle of α_N is s and the area between the inscribed regular polygon and the circle is S , thus

$$s = \frac{r^2}{2} \left(\alpha_N - 2 \cos \frac{\alpha_N}{2} \sin \frac{\alpha_N}{2} \right) \quad (1)$$

$$S = \frac{2\pi}{\alpha_N} s \quad (2)$$

Substituting s into S and using the area of the circle to divide S , we get

$$\delta = \frac{1}{\pi r^2} \left(\pi r^2 - \frac{Nr^2}{2} \sin \frac{2\pi}{N} \right) \quad (3)$$

when $N \rightarrow +\infty$, $\delta \rightarrow 0$. The more edges of the inscribed regular polygon there are, the closer the inscribed regular polygon is to a circle. Analogously, in the

EML method, the more equivalent conditions are set, the closer the mathematical model is to a continuous dynamic process.

3 Topology Optimization Model based on EML Method

Under multiple working conditions, the sensitivity of the same design variable is not the same under different working conditions, which means the relative density of the same element is not the same under all working conditions. One element may be deleted under one working condition whereas it may be retained under another working condition. It is a contradiction that the material of the same element is retained and deleted simultaneously. Therefore, in order to obtain an optimization result, a comprehensive analysis of multiple working conditions needs to be performed to decide the presence or absence of the element. Every working condition is usually seen as a single objective optimization function. By using a multi-objective optimization method, all working conditions are weighted to establish a comprehensive objective function. If, and only if, the relative density of the element is 0 under all working conditions, the element can be removed from the structure.

To make the optimization converge rapidly, the following basic assumptions are made: (1) the material of the brake disc is considered isotropic; (2) the sliding friction coefficient μ is constant during the sliding process; (3) the surface of the brake disc is an ideal flat plane.

During the braking process, the braking pressure changes over time. It is difficult to realize where the maximum braking pressure would be on the brake disc. Thus, in this study, the load in every equivalent working condition was set to the maximum brake pressure. Every equivalent working condition has the same effect as the maximum displacement in a dynamic process. Before and after equivalence, the primary requirement is that the brake disc should provide enough stiffness during the braking process. Therefore, the optimization of the brake disc in this paper mainly concerns the factor of rigidity. The comprehensive objective function $G(x)$ can be expressed as:

$$\begin{cases} \min G(x) = \sqrt{\sum_{i=1}^N [C_i(x)]^2} \\ \text{s.t.} \begin{cases} V \leq fV_0 \\ F_i = K_i U_i (i=1, 2, \dots, N) \\ 0 < x_{\min} < x \leq 1 \end{cases} \end{cases} \quad (4)$$

where x is the design variable, the relative density of each element. In order to avoid singularity, $x_{\min} = 0.001$. With an initial value of 1, an implicit iterative algorithm for the design variables is also established based on the interpolation scheme and the optimality criteria method. The variable i is the serial number of the working condition, and N is the total number of the EML working conditions. $C_i(x)$ is the compliance of the structure under the i -th working condition.

The response is set to rigidity and the objective function is set to minimized static rigidity; V is the volume of the optimized structure and V_0 is the initial volume of the structure; f is the volume percentage; F_i is the combined external force matrix of the structure at the i -th working condition; K_i and U_i are their corresponding stiffness matrices and displacement matrices. After the transformation with the above optimization model, the constraint $F_i = K_i U_i$ can be used for every working condition. So $i = 1, 2, \dots, N$. This has nothing to do with the continuous dynamic process. By using this mathematical model of topology optimization, the minimum value of $G(x)$ can be found.

4 Flow of Topology Optimization Using the EML Method

The flow of topology optimization using the EML method can be divided into the following steps:

1. Establish a three-dimensional model of the brake disc. Mesh the finite elements and set the constraints and load conditions.
2. Transform the contact pressure and the friction into multiple working conditions, then set the total number of working conditions to N_{\max} .
3. Set the initial serial number i of the working condition to 1.
4. Finite element analysis of the brake disc under the current working condition is carried out to obtain the displacement and compliance.
5. Analyze the sensitivity of the design variable.
6. Use the filtering techniques to prevent numerical instabilities such as porousness, checkerboards and mesh dependencies. The porousness and checkerboard phenomena make it difficult to reconstruct and manufacture an optimized structure. The mesh dependency will decrease the integrity of the structure. The grid filtering method used in this paper has been proposed by Sigmund [5]. In the post-processing stage, a convolution operator is introduced to weight-average the sensitivity of all the elements within a specified filter radius. The sensitivity information of the element is corrected and numerical instabilities are avoided.
7. Calculate the compliance of the structure under the current working condition.

8. Compare the current serial number N with the total number of working conditions N_{max} to judge whether the compliance calculation of all working conditions has been done or not. If $i \neq N_{max}$, then $i = i + 1$, Step (4) to Step (8) are repeated until $i = N_{max}$. If $i = N_{max}$, Step (9) is performed.
9. Determine whether the result meets the constraints or not. If it is satisfied, end the calculation. Otherwise, go on to the next iteration step and repeat Steps 3 to 10 until the convergence criterion is met.
10. End the calculation, output the relevant parameters, and perform model post-processing.

5 Finite Element Model and Determination of the Working Condition Number

5.1 Finite Element Model

A geometric model of the brake disc is established using the Pro/E 5.0 three-dimensional modeling software. The outer diameter of the brake disc is $D = 800$ mm, the inner diameter is $d = 200$ mm, and the thickness is $t_a = 40$ mm. The contact pressure and the friction are generated on both sides of the brake disc. It is symmetrical along the midline of the brake disc thickness. In order to reduce the amount of calculation in the optimization process, the optimization model is simplified to one half of the actual brake disc, $t = 20$ mm. The simplified schematic diagram is shown in Figure 3.

It is necessary to set the freedom of movement of all nodes along the thickness direction on the surface of the brake disc. After the EML method has been applied, the brake disc needs to be fixed. Therefore, all nodes on the surface of the brake disc shaft hole are connected to the center point in the actual brake disc shaft hole by using RBE2 rigid elements. The element type of the brake disc is a hexahedron. In addition, when the finite element model is set, the manufacturing constraints of the structure should also be considered. The brake disc optimized in this paper is a split type brake disc.

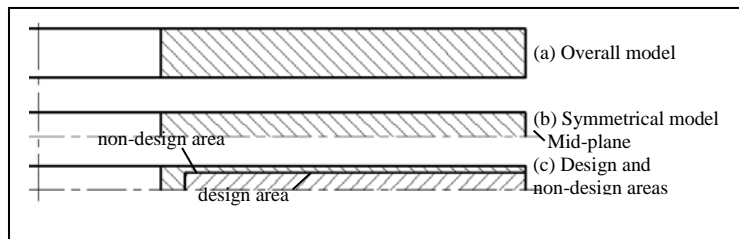


Figure 3 Simplified schematic of optimization model.

The assembly of the brake disc will be finished after forging each half of the brake disc, after which the friction surface will be manufactured. The volume fraction f in Eq. (4) is set to 80%. The established finite element model is shown in Figure 4.

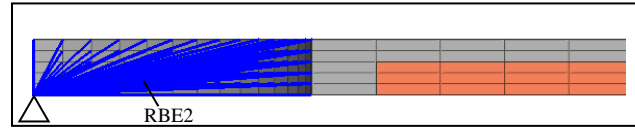


Figure 4 Finite element model. The blue liner elements (RBE2) are used to connect the center point and the nodes on the surface of the inner hole. The elements in gray belong to the non-design area and the orange ones belong to the design area.

The material used for the brake disc is Q345-B, its elastic modulus is $E = 2.06 \times 10^2 \text{ GPa}$, and Poisson's ratio is $\nu = 0.3$. The contact pressure $F_N = 17000 \text{ N}$ and the sliding friction coefficient of the friction pair composed of the brake disc/pad is $\mu = 0.3$. The established brake disc model is divided into two parts. One is the optimized area and the other is the non-optimized area. The non-optimized area includes the surface where the brake disc, the high-speed shaft and the contact surface between the brake disc and the brake pad.

5.2 Determination of the Working Condition Number

Based on the actual size of the brake pad and its layout style, the total number of feasible working conditions N_{\max} needs to be discussed. The brake discs with different numbers of brake pads are shown in Figure 5.

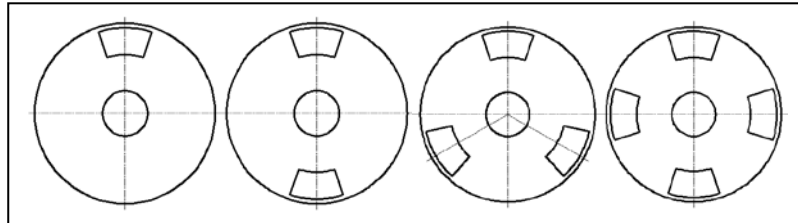


Figure 5 Layout style of the brake pads.

Under the constraint of meshing, the determination of the total number of feasible conditions N_{\max} with different layout styles of the brake pads can be calculated by Eq. (5):

$$N_{\max} = \frac{M}{mn} \quad (5)$$

where M is the number of the outermost elements of the brake disc. According to the established finite element model $M = 60$; the number of brake pads $m = 1, 2, 3, 4$; n is the number of elements between adjacent working conditions. The area of the brake pad is a sector area with an element number of 6×5 , so $n = 1, 2, 3, 4, 5, 6$. The total number of feasible working conditions N_{\max} can be calculated with Eq. (5), as shown in Table 1.

Table 1 Total Number of Feasible Working Conditions

Number of Brake Pads m	Number of Working Conditions N_{\max}
1	10, 12, 15, 20, 30, 60
2	5, 6, 10, 15, 30
3	4, 5, 10, 20
4	3, 5, 15

6 Optimization Process and Its Results

6.1 Optimization Process

After at least 80 iterations, the optimization result of each simulation group is obtained. Also, a structure that meets the requirement of the constraints is obtained. The iteration history of the objective function with different layout styles of the brake pads is shown in Figure 6. A decreasing objective function value means that the optimization process is stabilizing.

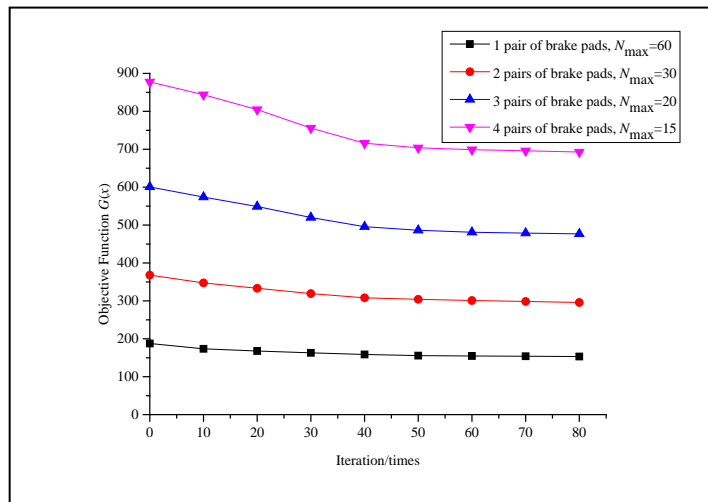


Figure 6 Iteration history of the objective function with different layout styles of the brake pads.

In Figure 6, as the pair number of brake pads increases, the initial value of the objective function increases almost linearly, but the dropping rate of the value become faster. When more brake pads are used during the braking process, the contact pressure and the friction on the brake disc become larger. This is the reason for the increasing initial value of the objective function. When 1 pair of brake pads is used, the line is almost a horizontal line. Along with the decrease of the total number of working conditions N_{\max} , the slope of the line increases. This means that the larger N_{\max} , the faster the optimization process reaches convergence.

6.2 Optimization Results

According to the flow of the topology optimization using the EML method, the topology optimization is completed according to the working conditions in Table 1. The optimization results are shown in Figures 7 to 10.

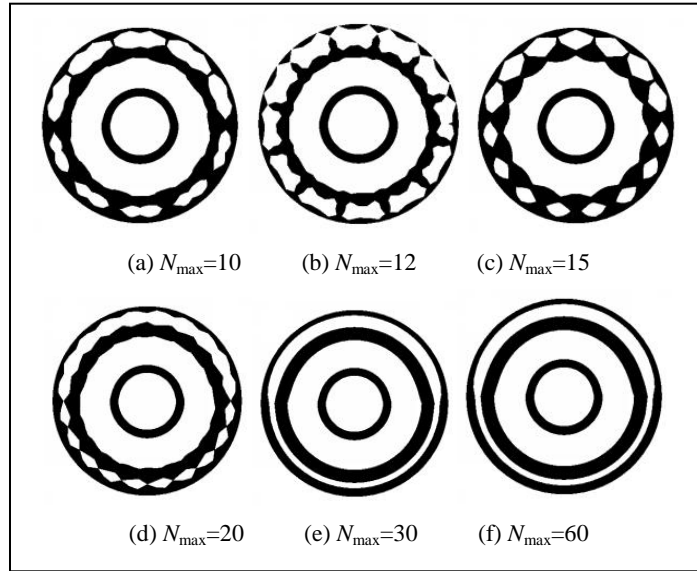


Figure 7 Optimization results of 1 pair of brake pads under different working conditions.

By using Eq. (3), we can calculate the optimization accuracy. Take one pair of brake pads as an example. When $N = 10, 12, 15, 20, 30, 60$, $r = 400$ mm, then $\delta = 0.0645, 0.0451, 0.0289, 0.0163, 0.0073, 0.0018$. From the value of δ , it can be found that the δ is becoming smaller while N is becoming larger.

No matter what kind of layout style is used, when the total number of working conditions N_{\max} is small, the number of holes in the topology results is affected

by N_{\max} , resulting in a decentralized structure, as shown in Figure 7(a)-(d), Figure 8(a)-(c), Figure 9(a)-(b), and Figure 10(a).

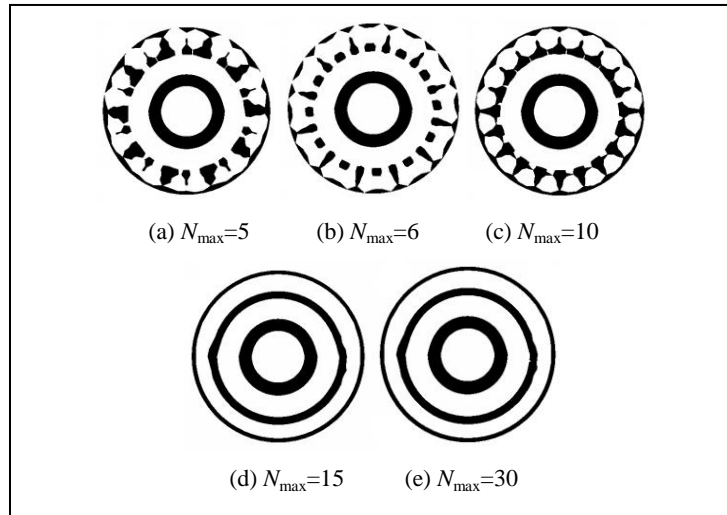


Figure 8 Optimization results of 2 pairs of brake pads under different working conditions.

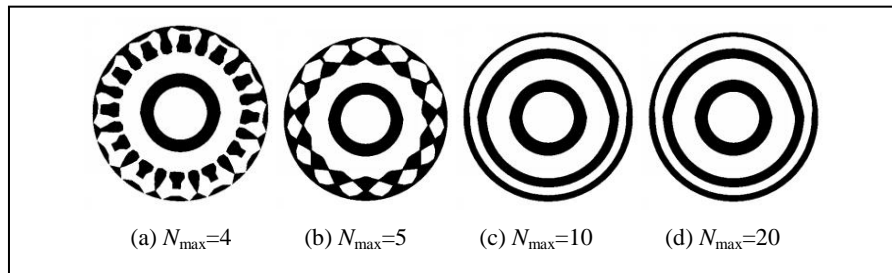


Figure 9 Optimization results of 3 pairs of brake pads under different working conditions.

When N_{\max} is small, the contact pressure and the friction are only applied to several areas on the brake disc. The effective area of the contact pressure and the friction is not continuous. There is no overlap between adjacent working conditions, resulting in a decentralized structure. With the increase of N_{\max} , the effective area of the contact pressure and the friction gradually becomes continuous, the overlap between adjacent working conditions gradually appears and the optimization result gradually becomes smoother.

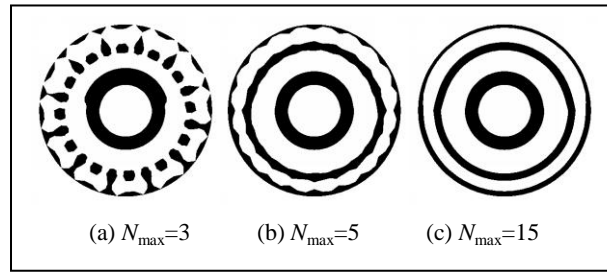


Figure 10 Optimization results of 4 pairs of brake pads under different working conditions.

The final optimization results are all three-annulus structures, as shown in the Figure 7(e)-(f), Figure 8(d)-(e), Figure 9(c)-(d), and Figure 10(b)-(c). The inner annulus is close to the non-optimized area and is far away from the friction area. It will be the innermost support material to resist the contact pressure and the friction. The space between the intermediate annulus and the outer annulus is the friction area. These two annuluses serve as the middle and outermost support material to prevent the brake disc from being deformed by the contact pressure and the friction.

Combining the optimization results and the manufacture process of the brake disc, the brake disc structure is reconstructed, as shown in Figure 11. The weight of the new structure is reduced by 57.95% compared to the initial structure. Moreover, before topology optimization, the maximum displacement of the brake disc under brake pressure and friction was 0.021 mm. However, after topology optimization with the EML method, the maximum displacement changed to 0.008 mm, which means the rigidity of the brake disc was improved after optimization.

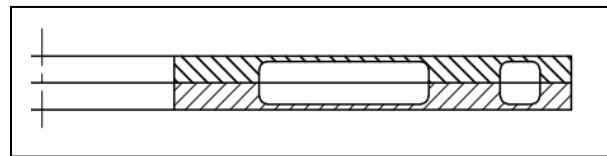


Figure 11 Reconstruction model of the brake disc.

7 Conclusions

In this study, a structural topology optimization method (EML) was developed to design the structure of a brake disc. The influence of different layout styles of the brake pads and the total number of feasible working conditions on the optimization results were analyzed.

The results showed that: (1) no matter what kind of layout style is used, when the total number of working conditions is small, the number of holes in the optimization result is affected by the total number of working conditions and the optimization result is a decentralized structure; (2) as the total number of working conditions is increases, the effective area of the contact pressure and the friction becomes continuous and the optimization result becomes smooth; (3) increasing the number of brake pads accelerates the appearance of overlap between adjacent working conditions, speeding up the convergence of the optimization; (4) the weight of the new structure was reduced by 57.95% compared to the initial structure by structural topology optimization using the EML method. It was proved that structural topology optimization using the EML method is efficient in optimizing the structure under dynamic load conditions.

Acknowledgements

The authors gratefully acknowledge the financial support from the National Natural Science Foundation of China under grant nos. 51675075 and 51475066 and from the Natural Science Foundation of Liaoning Province under grant no. 2015020114.

References

- [1] Bendsoe, M.P. & Kikuchi, N., *Generating Optimal Topologies in Structural Design Using a Homogenization Method*, Computer Methods in Applied Mechanics & Engineering, **72**(2), pp. 197-224, 1988.
- [2] Gao, J., Li, H., Gao, L. & Xiao, M., *Topological Shape Optimization of 3D Micro-Structured Materials Using Energy-Based Homogenization Method*, Advances in Engineering Software, **116**, pp. 89-102, 2018.
- [3] Noguchi, Y., Yamada, T., Izui, K. & Nishiwaki, S., *Topology Optimization for Hyperbolic Acoustic Metamaterials Using a high-Frequency Homogenization Method*, Computer Methods in Applied Mechanics & Engineering, **335**(2), pp. 419-471, 2018.
- [4] Fernandes, W.S., Greco, M. & Almeida, V.S., *Application of the Smooth Evolutionary Structural Optimization Method Combined with a Multi-Criteria Decision Procedure*, Engineering Structures, **143**(2), pp. 40-51, 2017.
- [5] Sigmund, O., *A 99 Line Topology Optimization Code Written in Matlab*, Structural and Multidisciplinary Optimization, **21**(2), pp. 120-127, 2001.
- [6] Min, S., Nishiwaki, S. & Kikuchi, N., *Unified Topology Design of Static and Vibrating Structures Using Multiobjective Optimization*, Computers & Structures, **75**(1), pp. 93-116, 2000.

- [7] Kunakote, T. & Bureerat, S., *Multi-objective Topology Optimization Using Evolutionary Algorithms*, Engineering Optimization, **43**(5), pp. 541-557, 2011.
- [8] Qu, J. & Su, H.F., *Optimization Design on Ventilated Disc Brake Based on surrogate Model Technology*, Engineering Mechanics, **30**(2), pp. 332-339, 2013.
- [9] Meng, G.Q., Zhang, Z.L. & Dai, R.Q., *Disc Brake Optimization Design and Finite Element Analysis*, Advanced Materials Research, **811**, pp. 325-330, 2013.
- [10] Zhang, X. & Kang, Z., *Dynamic Topology Optimization of Piezoelectric Structures with Active Control for Reducing Transient Response*, Computer Methods in Applied Mechanics & Engineering, **281**(11), pp. 200-219, 2014.
- [11] Ivarsson, N., Wallin, M. & Dan, T., *Topology Optimization of Finite Strain Viscoplastic Systems under Transient Loads*. International Journal for Numerical Methods in Engineering, 2018.
- [12] Liu, J., Wen, G. & Xie, Y.M., *Layout Optimization of Continuum Structures considering the Probabilistic and Fuzzy Directional Uncertainty of Applied Loads Based on the Cloud Model*, Structural & Multidisciplinary Optimization, **53**(9), pp. 1-20, 2015.
- [13] Liu, J., Wen, G. & Huang, X., *To Avoid Unpractical Optimal Design without Support*, Structural & Multidisciplinary Optimization, **56**(6), pp. 1589-1595, 2017.
- [14] Jeong, S.H., Lee, J.W., Yoon, G.H. & Choi, D.H., *Topology Optimization Considering the Fatigue Constraint of Variable Amplitude Load Based on the Equivalent Static Load Approach*. Applied Mathematical Modeling, **56**, pp. 626-647, 2018.